Chemical and structural characterization of $La_{0.5}Sr_{0.5}MnO_3$ thin films prepared by pulsed-laser deposition

P. Decorse, E. Quenneville, S. Poulin, M. Meunier,[a] and A. Yelon
Groupe des Couches Minces (GCM) and Department of Engineering Physics and Materials Engineering, Ecole Polytechnique de Montréal, C.P. 6079, succursale Centre-Ville, Montréal, Québec H3C 3A7, Canada

F. Morin
Institut de Recherche d'Hydro-Québec, Chimie et Environnement, 1800 Montée Lionel Boulet, Varennes, Québec J3X 1S1, Canada

(Received 16 June 2000; accepted 5 March 2001)

$La_{0.5}Sr_{0.5}MnO_3$ thin films were deposited onto sapphire substrates by means of the pulsed-laser deposition technique. These films were characterized by several techniques including x-ray diffraction, Rutherford backscattering spectrometry, energy-dispersive x-ray, atomic-force microscopy, scanning electron microscopy, and x-ray photoelectron spectroscopy (XPS). The cation ratios are the same in the deposited films as in the target. However, strontium segregation occurs at the film surface with an enrichment in this element compared to Mn and La, as shown by XPS. In addition, a clear correlation between the three different contributions which compose the O(1*s*) XPS signal and the Sr, La, and Mn surface concentrations has been established. Annealing the films at a sufficiently high-temperature produces the same crystal structure as in the target. © *2001 American Vacuum Society.* [DOI: 10.1116/1.1368200]

I. INTRODUCTION

Partial substitution of lanthanum by alkaline-earth metals in $LaBO_3$ (B=Co, Fe, Mn, Ni) perovskite oxides is known to improve the electrical, magnetic, and electrocatalytic properties of these compounds.[1–4] More specifically, the $La_{1-x}Sr_xMnO_3$ series has attracted considerable interest due to its application to cathode materials in solid oxide fuel cells (SOFCs).[5–11] For such an application, a good electrocatalytic activity for oxygen reduction and high electrical conductivity are required. In addition, chemical and mechanical compatibility with the yttria-stabilized zirconia electrolyte also needs to be considered. All these needs are fulfilled by $La_{0.5}Sr_{0.5}MnO_3$ (LSM5), which also has a low differential thermal expansion coefficient when used with stabilized zirconia.[5,8] One objective of the study of materials for reduced-temperature SOFCs is the use of thinner layers, at least for the solid electrolyte, in order to reduce the internal resistance drop within the cells. For cathode materials, it is advantageous to use thin films for the study of surface properties, and in order to obtain chemical equilibrium rapidly. Pulsed-laser deposition (PLD) is particularly well adapted to the deposition of such films due to its ability to transfer complex stoichiometry from the target to the film. This technique has already been used successfully for some lanthanum manganite-based compounds[12–19] of interest mainly for their magnetoresistance effect and electron-transport mechanisms.

The purpose of this work is the fabrication of LSM5 thin films by PLD, their physical characterization following various treatments, and the determination of chemical states at the surface of these films. The electrical properties of these films are further reported elsewhere.[20]

II. EXPERIMENT

The targets for the PLD process were prepared starting from a combustion-synthesized powder provided by Praxair. That powder had a nominal composition equivalent to $La_{0.50}Sr_{0.50}MnO_3$. Pellets were compressed first uniaxially, then cold isostatically to 300 MPa. These pellets were heated at 2 °C/min in pure oxygen to 1450 °C and then maintained at this temperature for 4 h. The sintered pellets, 19 mm in diameter by 4 mm in thickness, had a near-bulk density of 6.16 g/cm^3, as measured by an immersion technique. Single-crystal sapphire platelets from Kyocera were used as deposition substrates because of their surface quality and for their insulating properties, in view of the electrical measurements reported elsewhere.[20] They were oriented with their surfaces parallel to the *R* plane (1**1**02). Before deposition, the substrates were cleaned successively for 5 min in each of the following solvents: Opticlear™, acetone, propanol, and deionized water. They were then heated to 130 °C for 30 min to eliminate traces of water, immediately before being mounted into the vacuum-deposition chamber.

The background pressure in the PLD vacuum chamber was maintained at approximately 10^{-7} Torr. The sapphire substrates were placed on a rotating heated molybdenum sample holder (Johnsen Ultravac) at a distance of 5.5 cm in front of the target. A Kr–F excimer laser, model MPB AQX-150, generated pulses at a wavelength of 248 nm, with a 30 ns duration. The laser was focused onto the target, providing a 2 mm^2 elliptical spot. The energy density on the target was approximately 0.75 J/cm^2 and the pulse repetition rate was fixed at 30 Hz, leading to a film growth rate of about 10 nm/min. The LSM5 target was preablated for a few seconds

[a]Author to whom correspondence should be addressed; electronic mail: meunier@phys.polymtl.ca

in order to remove any surface impurities. The LSM5 films were deposited alternatively without heating or with nominal substrate temperatures T_S, equal to 550, 650, or 750 °C, the thermocouple readings being taken close to the sample holder. Film thicknesses measured by a Dektak profilometer ranged between 200 and 450 nm. Those thin films deposited at room temperature were annealed in air for 1 h at temperatures between 540 and 1040 °C. Heating and cooling rates were maintained at 2 °C/min.

Structural analysis was carried out using a Philips X'PERT diffractometer with Cu $K\alpha$ radiation for x-ray diffraction (XRD). Diffraction patterns were recorded in a $\theta/2\theta$ arrangement with 2θ varied in 0.03° steps between 20° and 60°. Patterns were indexed on the basis of an $R\bar{3}c$ hexagonal–rhombohedral cell. The various film morphologies were observed by means of optical microscopy, scanning electron microscopy (SEM), and a Topometrix TMX 2010 atomic-force microscope (AFM). Compositional profiles were investigated by Rutherford backscattering spectrometry (RBS) coupled to a Tandetron with a $^4He^{++}$ beam at 2.97 MeV. The resulting spectra were iterated through an appropriate simulation software. Chemical homogeneity across film surfaces was verified by energy-dispersive x-ray (EDX) microanalysis on a Philips XL20 scanning microscope equipped with an Oxford EDX spectrometer.

The surface chemical composition was analyzed using x-ray photoelectron spectroscopy (XPS) and a Vacuum Generators ESCALAB3 MK II x-ray photoelectron spectrometer with Al $K\alpha$ (1486.6 eV) and Mg $K\alpha$ (1253.6 eV) radiation at a working pressure of approximately 10^{-9} Torr. High-resolution core-level spectra were obtained at a pass energy of 20 eV, using 0.05 eV steps, giving a spectral resolution of about 0.7 eV. For quantitative analysis, atomic sensitivity factors were determined experimentally using the standard oxides La_2O_3, SrO, MnO, and MnO_2. Following either deposition or further annealing treatments, the samples were rapidly transferred to the analysis chamber and their spectra registered at room temperature without preliminary surface cleaning. The peaks for the La($3d$), Sr($3d$), Mn($2p$), and O($1s$) levels were recorded and the corresponding binding energies E_b normalized by using the C($1s$) level at 285.0 eV resulting from adventitious carbon at the surface. After linear-type background removal, the peaks were separated using an in-house, nonlinear, least-mean-squares program.

III. RESULTS AND DISCUSSION

A. Volume characterization

The LSM5 targets with an average grain size of about 4 μm in diameter were single phase and homogeneous throughout the bulk, as observed by XRD and EDX. The corresponding diffraction pattern can be indexed on the basis of the hexagonal–rhombohedral structure ($R\bar{3}c$), in agreement with the literature.[5,21] LSM5 thin films deposited at room temperature are amorphous and electrically insulating. They are dense, adherent, and relatively feature free with few irregularities at the 30–40 nm level, as detected by AFM.

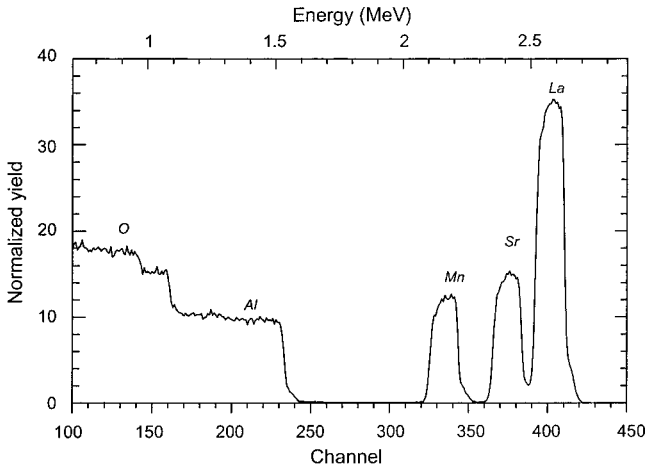

FIG. 1. RBS spectrum of a LSM5 film deposited at 550 °C.

Both room- and high-temperature-deposited films exhibit about the same chemical composition, as confirmed by EDX and RBS measurements. X-ray mapping of the samples shows no significant variation of chemical composition across the surface. Chemical composition of the films is within ±5% of the target composition for any element, which corresponds to the EDX experimental uncertainty in the present case. The RBS spectrum for chemical profiling of a LSM5 high-temperature-deposited film is shown in Fig. 1. Two oxygen contributions are present, the first for the LSM5 film, and the second for the underlying sapphire substrate. Sr and La peaks increasingly overlap with larger film thicknesses. Iterative simulation of the RBS spectra leads to $La_{0.51}Sr_{0.47}Mr_{1.03}O_{3.03}$ for the room-temperature film and to $La_{0.51}Sr_{0.49}Mr_{0.93}O_{2.98}$ for the film deposited at 550 °C. These compositions are close to the target formulation, taking into account the experimental uncertainty, which is around 5%.

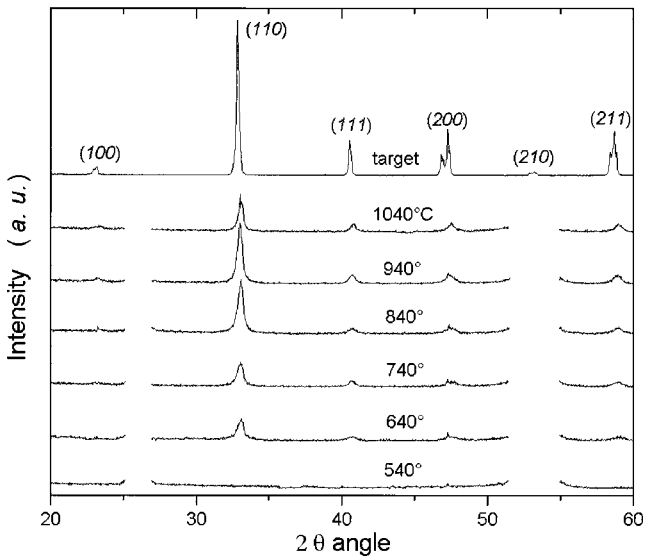

FIG. 2. X-ray diffraction patterns of LSM5 films deposited at room temperature and annealed in air at various temperatures. The diffraction pattern of a LSM5 target with pseudocubic indices is also given for comparison.

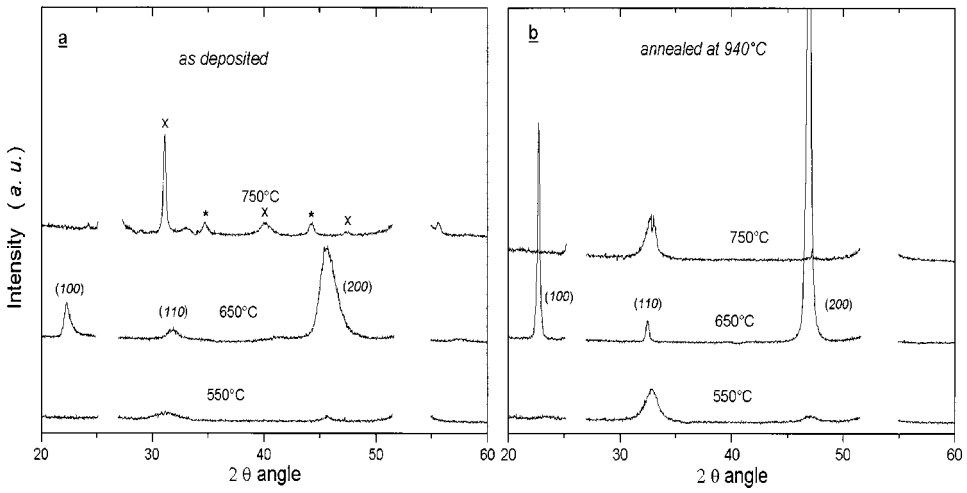

FIG. 3. X-ray diffraction patterns of LSM5 thin films deposited at 550, 650, and 750 °C, before and after being annealed in air at 940 °C. Pseudocubic indices are used. Asterisks indicate unidentified phases.

This is in good agreement with the chemical homogeneity already attributed to the results reported earlier.[22] Further measurements on high-temperature-annealed samples give no indication of any significant composition variations within the films. Thus, no measurable interdiffusion between thin films and the substrate took place upon annealing.

LSM5 is rhombohedric with overlapping peaks closely related to a cubic structure. For the sake of simplicity within the present discussion, pseudocubic indices are used. The two gaps within the x-ray diagrams for thin films correspond to the two strong reflections from the sapphire substrates. The room-temperature-deposited films remain amorphous after annealing for 1 h at 540 °C, as shown in Fig. 2. But, recrystallization readily occurs at 640 °C with peaks typical of LSM5. Further increasing the annealing temperature up to 840–940 °C leads to increasing recrystallization. There is only a slight improvement in the diffraction patterns between the two highest temperatures. No second phase and no preferential orientation are detected at this stage. The pattern for a film annealed at 1040 °C suggests degradation, although the signal remains too faint to show any new reaction products which may be formed between the LSM5 films and the substrates. Such degradation is more evident in the SEM images.

Deposition onto substrates heated to 550 °C and above yields some cristallinity immediately. In Fig. 3(a), two weak, broad peaks, corresponding to the LSM5 (110) and (200) pseudocubic planes are visible at $T_S = 550$ °C. At $T_S = 650$ °C, an additional peak, corresponding to the (100) pseudocubic plane in LSM5, appears and the relative intensity of the (200) peak increases considerably. We attribute the strong preferred orientation within this film to the sapphire substrate, which was the only one within this study with an orientation different from the *R* plane. The slight shifts of the peaks at $T_S = 550$ and 650 °C towards lower angles may be attributed to a lower degree of cristallinity of these films before being further annealed. At $T_S = 750$ °C, the peaks marked with an ''x'' should still pertain to the LSM5 perovskite phase. Nonetheless, new unidentified peaks are indicative of a partial decomposition of this compound. The partial formation of $(La,Sr)_2MnO_4$ is most probable but remains to be confirmed. Thus, 750 °C is an upper limit for producing LSM5 films without providing oxygen enrichment of the surrounding atmosphere in the PLD chamber. Annealing of the high-temperature-deposited LSM5 films in air at 940 °C considerably improves their cristallinity, as shown in Fig. 3(b). The preferred orientation of the films deposited at 650 °C is further emphasized. The films deposited at 750 °C also revert to the diffraction pattern normally expected for LSM5.

The room-temperature-deposited films are generally feature free when viewed by SEM and AFM. Annealing produces roughening of the surface, corresponding to recrystallization and to grain-boundary formation. At 640 °C, grains are barely perceptible at the surface, but become more visible with increasing annealing temperature. At 940 °C, grains are generally uniform in size, as shown in Fig. 4, with an average diameter of 240 nm. Small crystallites appear as an additional feature in Fig. 4. They reach a height of, at most, 260 nm as measured by AFM. They are only found after

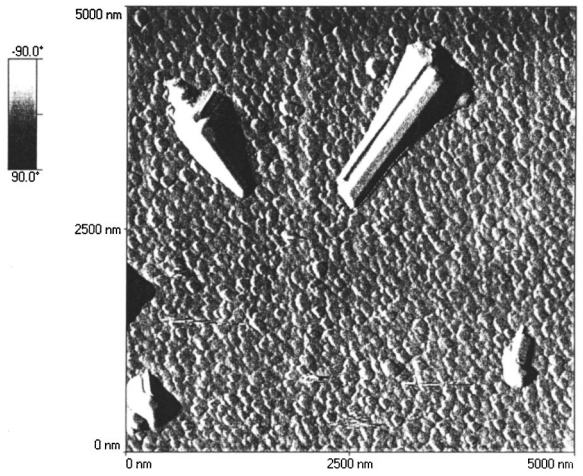

FIG. 4. Surface morphology of a room-temperature-deposited film annealed in air at 940 °C.

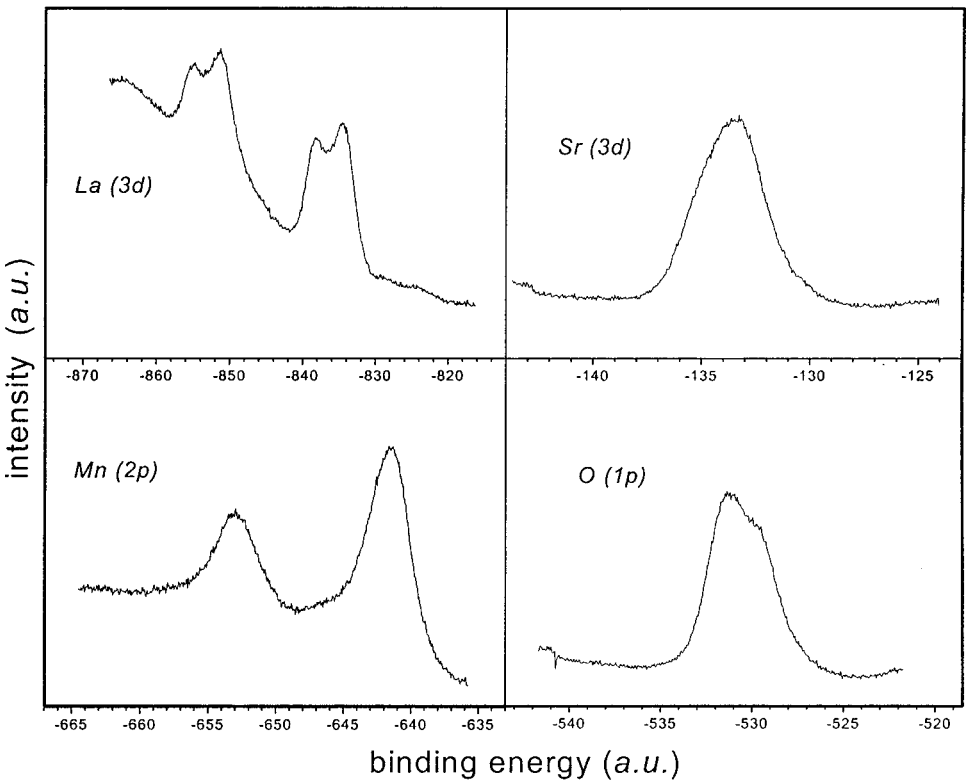

FIG. 5. XPS spectra for the various elements of a room-temperature-deposited LSM5 film.

annealing at high temperature and they remain generally dispersed throughout the surface. They should proceed from the film tendency to produce larger crystallites at higher temperature. No segregation is indicated by EDX measurements. The emergence of crystallites from the surface is attributed to a common tendency for facetting in ceramics at higher temperatures and, eventually, to the local growth of some preferred orientations. Finally, some cracking is observed in films annealed at 940 and 1040 °C. This phenomenon is related to the mismatch between the film and the substrate thermal expansion coefficients.

B. XPS measurements

XPS spectra for the various elements at the surface of the room-temperature-deposited films are shown in Fig. 5. Surface concentrations were obtained from the spectra for various deposition temperatures and annealing treatments. These results appear in Table I. Variations in the La/Mn ratios are not very significant. The expected accuracy typical of XPS analyses (5%) leads to a 10% uncertainty on the ratios. In contrast, strontium is strongly segregated at the surface of LSM5 films, in agreement with previous observations on bulk samples.[23] This is true for all samples, deposited at room temperature, further annealed at high temperature, or deposited onto heated substrates. The highest segregation of strontium is encountered at a substrate deposition temperature of 750 °C. This is the condition which yields a crystal structure different from the one expected for LSM5.

Additional information on surface chemical states on LSM5 films may be obtained from the shapes and binding energies of the XPS peaks. Two C($1s$) peaks are present on the samples. The first, which is always present, is at 285.0 eV, and corresponds to the well-known ''adventitious carbon'' peak, produced by atmospheric hydrocarbons. The second, which is not systematically present, is at 289.3 eV. This energy corresponds to another atmospheric hydrocarbon peak, and to carbonate, so that either or both may be present.

The core and satellite peaks for La($3d$) remain the same for all samples. The corresponding binding energies are in good agreement with reported values, for example, 834.0

TABLE I. Surface composition (at. %) and cationic ratios of LSM5 films as obtained by XPS.

Elements	O	La	Sr	Mn	La/Mn	Sr/Mn
Nominal	60	10	10	20	0.5	0.5
RT	63.0	7.3	16.4	13.3	0.55	1.2
RT+840 °C	60.5	10.4	14.3	14.8	0.70	1.0
RT+940 °C	62.0	9.0	15.5	13.5	0.67	1.1
T_S=550 °C	57.6	7.4	18.9	16.1	0.46	1.2
=650 °C	57.7	9.4	15.9	17.0	0.55	0.9
=750 °C	56.9	8.6	22.8	11.7	0.74	1.9

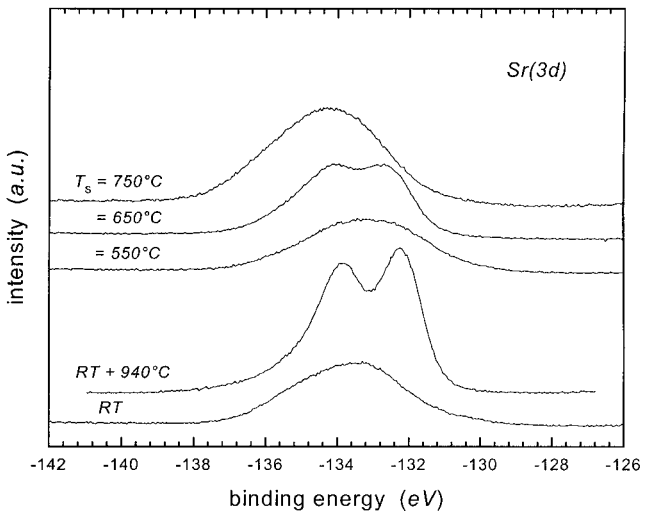

FIG. 6. Evolution of the XPS Sr($3d$)-level spectrum of various LSM5 films with different thermal histories.

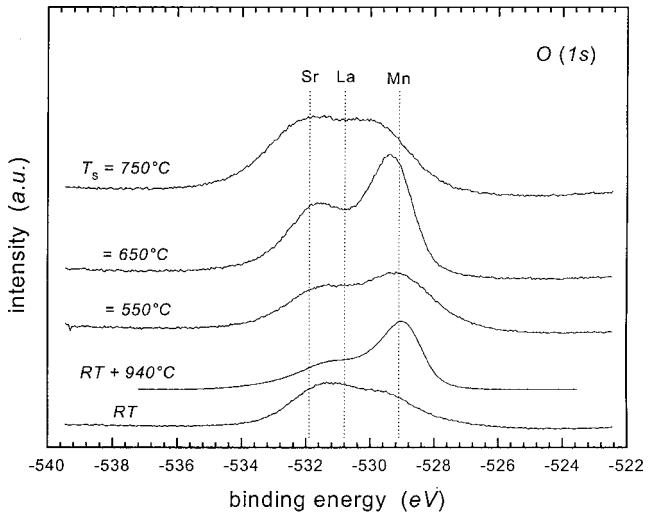

FIG. 7. Evolution of the XPS O($1s$)-level spectrum of various LSM5 films with different thermal histories. The binding energies of electrons in oxides of Sr, La, and Mn are also indicated.

± 0.2 eV for La($3d_{5/2}$).[24] Energy difference ΔE between the ($3d_{3/2}$) and ($3d_{5/2}$) levels is also similar for all samples, and is approximately equal to 17 eV. The binding energies and multiplet splitting agree well with reported values for La^{3+} in La_2O_3.[25–27] Binding energies for the Mn($2p_{1/2}$) and Mn($2p_{3/2}$) levels are equal to 653.0 and 641.4 eV for most samples, in close agreement with the Mn($2p$) levels reported by Evans and Raftery for similar compounds.[28] Moreover, the binding energy increases slightly with increasing deposition temperature. This suggests that Mn is further oxidized at high temperature, i.e., that the Mn^{4+}/Mn^{3+} ratio increases.

The Sr spectrum, as shown in Fig. 6, contains two features. The first is a doublet at 132 eV binding energy, with a separation of 1.7 eV between the Sr($3d_{3/2}$) and Sr($3d_{5/2}$) peaks. The second is a broad peak, whose center is at 133–135 eV, depending upon the sample. In order to provide an interpretation of these spectra, we note that correlations can be made with the data of Table I, and with the XRD data. Comparing the as-deposited films, we note that the film deposited at 650 °C, which shows a diffraction pattern corresponding to perovskite, but a rather low-Mn surface concentration, exhibits a barely resolved doublet. The film deposited at 550 °C, which shows a high-Mn concentration, but weak diffraction pattern, shows no doublet, but exhibits a broad peak centered at relatively low binding energy. The film deposited at 750 °C, which has the lowest Mn concentration, and an XRD pattern corresponding to nonperovskite phases, exhibits the broad peak with the highest binding energy. Finally, the film annealed at 940 °C, which shows a good perovskite diffraction pattern, and average Mn concentration, exhibits the clearest doublet, at the lowest binding energy.

We propose that the XPS spectra may be interpreted as resulting from two, or possibly three, components. It is known[29–31] that the binding energy for Sr in SrO is at about 135 eV, and is at about 133 eV for $SrCO_3$. It has also been reported[32] that these, and other components, are difficult to resolve. We believe that much of the intensity of the broad peak is due to SrO, and that the peak shifts to higher binding energies as this component becomes more abundant. There may be some contribution from the carbonate as well, but this is difficult to demonstrate. We suggest that the low-binding-energy doublet is due to $SrMnO_3$ in the crystalline perovskite, and that the low-energy component in the broad peak is either the doublet, which cannot be resolved from the other components, or $SrMnO_3$ in amorphous form. The segregation of Sr at the surface can be understood from the above analysis as arising from its high reactivity, so that it forms surface oxides if it is not incorporated into the perovskite.

This interpretation is supported by analysis of the O($1s$) spectra, shown in Fig. 7. All of the spectra were deconvoluted into three peaks. For all samples, the positions of the three peaks were at 529.0, 530.8, and 531.9 ± 0.3 eV. Liang and Weng,[33] who studied $La_{0.3}Sr_{0.7}MnO_3$ and related compounds, have attributed peaks at these positions to surface oxygen associated with Mn, La, and Sr. Similar spectra have been found for other substituted ABO_3 compounds.[19,24,25] We follow this attribution, which is consistent with our analysis of the Sr spectra, as shown in Fig. 7. In so doing, we have effectively assumed that the contributions to the O($1s$) spectra, of O–C at 533.9 eV, O═C in CO_3 near 532 eV, H_2O at 533 eV, –OH at 531–533 eV, and weakly bonded O_2 at 529 eV, are all small.

On the basis of the proposed attributions, we may see that the variation of the peak intensities in the O($1s$) spectra between samples correlate well with the variations in the peak intensities and positions in the Sr spectra. That is, the samples deposited at 650 °C or annealed at 940 °C, which show strong peaks for O associated with Mn, show the doublet that we have attributed to Sr in $SrMnO_3$. The sample deposited at 750 °C, which shows the strongest signal of O bonded to Sr, and almost no O bonded to Mn, shows no

perovskite phase in XRD, and the most strongly bonded Sr signal, which we attribute to SrO. Between the two extremes, the O binding energy increases as the Sr binding energy increases, as should be expected. Thus, the results of the different measurements are consistent.

IV. CONCLUSIONS

$La_{0.5}Sr_{0.5}MnO_3$ thin films have been fabricated by pulsed-laser deposition with and without substrate heating. As a whole, the target composition is successfully transferred to the films. Thin films deposited at room temperature are amorphous. Following annealing in air at temperatures above 540 °C, the resulting films crystallize into the LSM5 perovskite structure. According to the XPS results, the surface composition is different from the bulk, the strontium-to-manganese ratio at the surface being significantly higher than within the bulk. A correlation exists between the different contributions to the O(1*s*) level and the Sr, La, and Mn surface concentrations.

ACKNOWLEDGMENTS

The authors wish to thank the Natural Sciences and Engineering Research Council of Canada (NSERC) and the Hydro-Quebec Research Institute (IREQ) for financial support. The authors also acknowledge Dr. Abdeltif Essalik for useful discussions and Jean-Paul Lévesque for technical support.

[1]L. G. Tejuca, J. L. C. Fierro, and J. M. Tascon, Adv. Catal. **36**, 237 (1989).
[2]P. J. Gellings and H. J. M. Bouwmeester, Catal. Today **12**, 1 (1992).
[3]A. Urushibara, Y. Moritomo, T. Arima, A. Asamitsu, G. Kido, and Y. Tokura, Phys. Rev. B **51**, 14103 (1995).
[4]W. Feduska and A. O. Isenberg, J. Power Sources **10**, 89 (1983).
[5]A. Hammouche, E. Siebert, and A. Hammou, Mater. Res. Bull. **24**, 367 (1989).
[6]O. Yamamoto, Y. Takeda, R. Kanno, and T. Kojima, in *Proceedings of the First International Symposium on Solid Oxide Fuel Cells*, edited by S. C. Singhal (The Electrochemical Society, Pennington, NJ, 1989), Vol. 89-11, p. 242.
[7]H. U. Anderson, Solid State Ionics **52**, 33 (1992).
[8]H. Yamada and H. Nagamoto, in *Proceedings of the 3rd International Symposium on Solid Oxide Fuel Cells*, edited by S. C. Singhal and H. Iwahara (The Electrochemical Society, Pennington, NJ, 1993), Vol. 93-4, p. 213.
[9]Z. Li, M. Bchruzi, L. Fucrst, and D. Stöver, in *Proceedings of the 3rd International Symposium on Solid Oxide Fuel Cells*, edited by S. C. Singhal and H. Iwahara (The Electrochemical Society, Pennington, NJ, 1993), Vol. 93-4, p. 171.
[10]B. Gharbage, F. Mandier, H. Lauret, and T. Pagnier, Solid State Ionics **82**, 85 (1995).
[11]H. Tagawa, N. Mori, H. Takai, Y. Yonemura, H. Minamiue, H. Inaba, J. Mizusaki, and T. Hashimoto, in *Proceedings of the 5th International Symposium on Solid Oxide Fuel Cells*, edited by U. Stimming, S. C. Singhal, H. Tagawa, and W. Lehnert (The Electrochemical Society, Pennington, NJ, 1997), Vol. 97-40, p. 785.
[12]S. Jin, M. McCormack, T. H. Tiefel, and R. Ramesh, J. Appl. Phys. **76**, 6929 (1994).
[13]A. Gupta, T. R. McGuire, P. R. Duncombe, M. Rupp, J. Z. Sun, W. J. Gallagher, and G. Xiao, Appl. Phys. Lett. **67**, 3494 (1995).
[14]J. F. Lawler, J. M. D. Coey, J. G. Lunney, and V. Skumryev, J. Phys.: Condens. Matter **8**, 10737 (1996).
[15]A. Endo, M. Ihara, H. Komiyama, and K. Yamada, Solid State Ionics **86-88**, 1191 (1996).
[16]M. Jaime, M. B. Salamon, M. Rubinstein, R. E. Treece, J. S. Horwitz, and D. B. Chrisey, Phys. Rev. B **54**, 11914 (1996).
[17]Y. Konishi, M. Kasai, M. Izumi, M. Kawasaki, and Y. Tokura, Mater. Sci. Eng., B **56**, 158 (1998).
[18]A. Machida, Y. Moritomo, and A. Nakamura, Phys. Rev. B **58**, R4281 (1998).
[19]B. Mercey, P. A. Salvador, W. Prellier, T. D. Doan, J. Wolfman, J. F. Hamet, M. Hervieu, and B. Raveau, J. Mater. Chem. **9**, 233 (1999).
[20]E. Quenneville, P. Decorse, M. Meunier, F. Morin, and A. Yelon in *Proceedings of the Symposium on Solid State Ionic Devices*, edited by E. D. Wachsman, J. Akridge, M. Liu, and N. Yamazoe (The Electrochemical Society, Pennington, NJ, 1999), Vol. 99-13, p. 218.
[21]R. Millini, M. F. Gagliardi, and G. Piro, J. Mater. Sci. **29**, 4065 (1994).
[22]J. T. Cheug and H. Sankur, CRC Crit. Rev. Solid State Mater. Sci. **15**, 63 (1988).
[23]P. Decorse, G. Caboche, and L. C. Dufour, Solid State Ionics **117**, 161 (1999).
[24]S. H. Overbury, P. A. Bertrand, and G. A. Somorjai, Chem. Rev. **75**, 587 (1975).
[25]K. Tabata, I. Matsumoto, and S. Kohiki, J. Mater. Sci. **22**, 1882 (1987).
[26]N. Gunasekaran, S. Rajadurai, J. J. Carberry, N. Bakshi, and C. B. Alcock, Solid State Ionics **73**, 289 (1994).
[27]N. Gunasekaran, N. Bakshi, C. B. Alcock, and J. J. Carberry, Solid State Ionics **83**, 145 (1996).
[28]S. Evans and E. Raftery, Clay Miner. **17**, 477 (1982).
[29]*Handbook of X-Ray Photoelectron Spectroscopy* (Perkin-Elmer, Eden Prairie, MN, 1992).
[30]A. B. Christie, J. Lee, J. Sutherland, and J. M. Walls, Appl. Surf. Sci. **15**, 224 (1983).
[31]H. Van Doveren and J. A. Verhoeven, J. Electron Spectrosc. Relat. Phenom. **21**, 265 (1980).
[32]V. Young and T. Otagawa, Appl. Surf. Sci. **20**, 228 (1985).
[33]J. Liang and H. Weng, Ind. Eng. Chem. Res. **32**, 2563 (1993).